26th EPS Conf. on Contr. Fusion and Plasma Physics, Maastricht, 14 - 18 June 1999 ECA Vol.23J (1999) 1217 - 1220

Radial Displacement of Pellet Ablation Material in Tokamaks Due to the Grad-B Effect

P.B. Parks, W.D. Sessions,[1] L.R. Baylor[2]

General Atomics, P.O. Box 85608, San Diego, California 92186-5608, USA

[1]Tennessee Technical University,,Cookeville, Tennessee.
[2]Oak Ridge National Laboratory, Oak Ridge, Tennessee.

Recently, Lang et al. drew attention to the possibility of enhancing fuel penetration by injecting D_2 pellets from the inside wall or high-field side of ASDEX-U [1]. Since then, new experimental findings on DIII–D confirm that inside launched pellets deposit fuel closer to the interior of the plasma, and well beyond the pellet range of throw [2]. This apparent movement of the ablated and ionized pellet substance towards the low-B-field or large-R side of the tokamak can be attributed to uncompensated ∇B and curvature drifts induced by the $1/R$ variation in the toroidal field strength. Compared to the surrounding plasma medium, the ionized part of the pellet ablation cloud is a mildly diamagnetic object with a higher internal magnetic β and guiding center drift current density. The characteristic β on the sonic surface $r = r_{*'} = 1.6 r_p$, is $\beta_{*'} = 4.3\times10^3 \beta_\infty (W T_{e\infty}^2 / n_{e\infty} r_p \ln\Lambda_{en})^{1/3}$, where r_p is the pellet radius, W is the pellet atom mass in amu, $T_{e\infty}$, $n_{e\infty}$, β_∞ are respectively the electron temperature, electron density, and β of the surrounding plasma, $\Lambda_{en} = 2T_{e\infty}/7.5$, and eV-cm units are used. For example, the experimental parameters for inside launched deuterium pellets in DIII–D are: B = 30 kG, $T_{e\infty}$ = 1.3 keV, $n_{e\infty} = 7\times10^{13}$ cm^{-3} and r_p = 0.05 cm, which gives β_∞ = 0.008, and $\beta_{*'}$ = 0.19. The cloud pressure and β decays by radial expansion. Simultaneously, the cloud becomes ionized and conducting with distance until at some point the magnetic field force impedes the transverse motion and funnels the outflow into a long ionized "shielding channel." Inasmuch as the ionized channel β falls considerably below $\beta_{*'}$ but still remains higher than β_∞, a polarization electric field appears inside, causing this part to move across the B field ahead of the pellet.

The observed pellet oscillation-striations, driven by a rotation instability [3], separate the shielding channel from the pellet, and breed a sequence of typically 20 or more "detached cloudlets" along the pellet trajectory. We assume each cloudlet carries off the ablated mass contained in the shielding channel at the moment of its birth, and inherits the dimensions and parallel flow profiles of the shielding channel. Subsequently, the cloudlet expands along the field lines while drifting as a whole across the magnetic field.

Parallel Flow Model for the Attached Shielding Channel

We assume constant area cross section $A(s) = \pi r_\perp^2$, and borrow standard 1-D duct flow expressions that relate the flow variables at one location with Mach number $M = v_\parallel / c_s$ to their corresponding values at the sonic M =1 channel-plasma interfaceface, $s = L_c$. In the pellet frame of reference, the toroidal drift effect causes the shielding channel to bend gradually with distance s in the direction of the major radius [4]. The axial distance where the centroid of the channel has shifted by an amount equal to its radius sets the effective shielding length $L_c \sim (r_\perp R)^{1/2}$.

Internal heating is based on a kinetic treatment for the deposition of energy by plasma electrons incident on the cloud with a half-space Maxwellian distribution. In passing through a column density $\tau = \int n ds$, the energy flux carried by the incident electrons, q, is attenuated by the amount $\eta \equiv q/q_\infty = 0.5 u K_2(u^{1/2})$, in which $u = \tau/\tau_\infty$, $\tau_\infty(\text{cm}^{-2}) = 2.24\times10^{12} T_{e\infty}^2(\text{eV}) / \ln\Lambda_{ee}$, K_2 is a Bessel function, and $q_\infty = (2/\pi m_e)^{1/2}$

$n_{e\infty} T_{e\infty}^{3/2} \exp[-\Delta\Phi / T_{e\infty}]$, with the sheath potential drop [3] at the channel-plasma interface being $\Delta\Phi \cong 1.8 T_{e\infty}$. All the flow profiles in the shielding channel are uniquely determined by specifying only two channel entrance properties, M_0 and n_0. From mass conservation: $G = 2\pi r_\perp^2 m_i n_0 M_0 c_{s0}$, and the known scaling laws for the ablation rate G, we can infer n_0

$$n_0 = \frac{1.07\times 10^3 W^{1/3} n_{e\infty}^{2/3} T_{e\infty}^{11/3}}{r_p^{4/3} \kappa_c^4 M_0^2 B_\infty^2 (\mathrm{kG}) \beta_0 (\ln \Lambda_{en})^2} \quad , \tag{1}$$

The scaling of the normalized channel radius $\kappa_c = r_\perp / r_p$ is not yet resolved, but experiments [5] and theory [6] are in reasonable agreement, suggest that κ_c ~ 10 to 20. The value of M_0 is also not yet clear, however, we note that a shock front must exist in the transition region between the sonic surface and the channel entrance and hence M_0 is restricted to the range [(3/7)$^{1/2}$, 1]. The "heating quotient" $\hat{Q} = q_\infty / m_i n_0 \bar{c}_0^3$, with entrance sound speed $\bar{c}_0 = (2T_0 / m_i)^{1/2}$, can be obtained from global enthalpy balance considerations, including the latent energy of ionization, I_i = 13.6 eV/ion, and assuming that ionization is nearly complete at the channel entrance, so that T_0 ~ 2 eV

$$\hat{Q} = 2\gamma^{3/2} \frac{(1+\gamma M_0^2)^2}{M_0 (1+\gamma)^2} \left(1 + \frac{I_i \Theta_0}{4\gamma T_0} \right) \quad . \tag{2}$$

In view of the mild assumptions about the inlet Mach number M_0, the numerical value for $\hat{Q}$ is relatively constant; we take $\hat{Q} \approx 5$ in subsequent calculations. The inlet channel β_0 initializes the cloudlet β at the midplane, and it can be estimated by eliminating n_0 between Eq. (1) and the value of the heating quotient from Eq. (2).

Parallel Flow Model for the Detached Cloudlet

A 1-D Lagrangian fluid model is used to describe the cloudlet expansion along the magnetic field lines. The boundary condition at the cloudlet-plasma interface is that the pressure in the last Lagrangian cell is equal to the plasma pressure. We only follow the early time evolution of the cloudlet up until the pressure in each fluid element has relaxed to the background plasma pressure. During this time the cloud temperature is increasing but typically remains well below the background plasma temperature so that the Fokker-Planck based heat attenuation model of the previous section remains valid.

The flow dynamics depend on only two dimnsionless parameters: the "normalized absorption coefficient" $\Sigma_0 = n_0 L_c / \tau_\infty$, and the initial cloud-to-plasma pressure ratio at the midplane $p_0 / p_\infty = \beta_0 / \beta_\infty$. Figure 1 displays the pressure profiles for different times. Initially the expansion is counteracted by the background pressure causing a slight elevation of the interior pressure above its initial value. Later the profile relaxes and eventually becomes homogeneous within the cloud at the value of the background pressure. Figure 2 is a plot of the dimensionless cloud length $z_c(t) / L_c$ versus time $\tilde{t} = t / (L_c / \bar{c}_0)$.

Cross-Field Drift Dynamics for the Detached Cloudlet

Having quantified the pressure relaxation process in the expanding cloudlet, we turn now to the motion of the cloudlet as a whole across the magnetic field. In response to the induced electric field inside the cloud it drifts acrof oss the magnetic field at the velocity $v_\perp = \hat{z} \times \nabla\varphi / B$ where $\hat{z}$ is the unit vector in the direction the magnetic field. The problem is to calculate the perturbed electrostatic potential $\varphi(r, \vartheta, t)$ inside and outside the moving cloudlet. We use a cylindrical coordinate system attached to the cloudlet at time t, with $z = 0$ locating the midplane of the system at that time. The potential variation in the z-direction is neglected because of finite parallel conductivity. Hence the transverse cloud motion can be decoupled from the previously treated parallel expansion dynamics. The transverse one-fluid

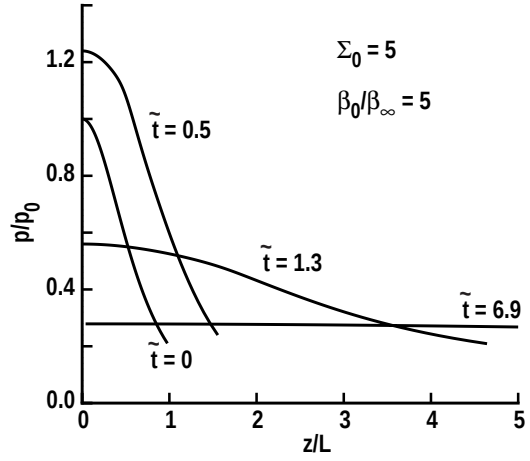

Fig. 1. Axial pressure profiles in detached cloudlet at different sound times: $\tilde{t} = t / (L_c / \bar{c}_0)$.

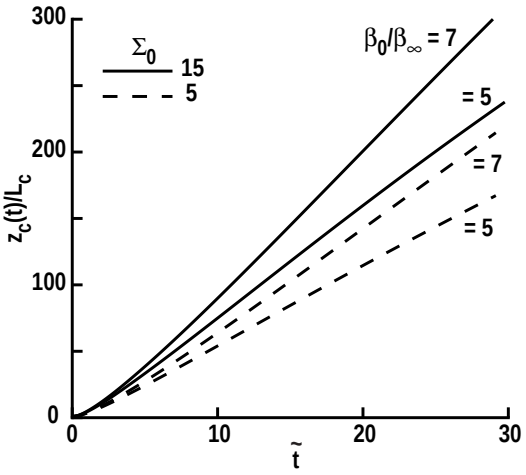

Fig. 2. Cloudlet half-length versus time.

momentum balance equation is

$$\rho \frac{D\mathrm{v}_\perp}{Dt} = J \times B - \nabla_\perp p + \frac{2p}{R}\hat{x} \tag{3}$$

where $D/Dt = \partial/\partial t + \mathrm{v}_\perp \cdot \nabla$ is the convective derivative. The last term in Eq. (3) simulates the effect of magnetic curvature, which is sometimes employed when the magnetic field is otherwise treated as being uniform, and the unit vector $\hat{x} = \hat{r}\cos\vartheta - \hat{\vartheta}\sin\vartheta$ points in the direction of the major radius. Taking the cross product of Eq. (3) with $\hat{z}$ gives the transverse current density, and charge continuity equation $\nabla \cdot \vec{J} = 0$ then yields

$$\nabla_\parallel \cdot \vec{J}_\parallel - \frac{2\sin\vartheta}{BR}\frac{\partial p(r,z,t)}{\partial r} - \frac{\rho}{B^2}\frac{D\nabla_\perp^2\varphi}{Dt} = 0 \quad . \tag{4}$$

By symmetry, the parallel current density must be zero at $z = 0$, so that an integration of Eq. (4) over the half-length of the cloud, $0 < z < z_c(t)$ yields

$$J_\parallel(z_c) - \frac{2\sin\vartheta}{BR}\int_0^{z_c}\frac{\partial p(r,z,t)}{\partial r}dz - \frac{\Sigma_\rho}{B^2}\frac{D\nabla_\perp^2\varphi}{Dt} = 0 \tag{5}$$

where $\Sigma_\rho = \int \rho dz$. The parallel current density emitted from the end of the cloudlet $J_\parallel(z_c)$ must match that carried by the Alfven wave sent out into the plasma $J_\parallel = -\mu_0^{-1}\nabla_\perp^2 A_\parallel$. Since $E_\parallel = -ik_\parallel\varphi + i\omega A_\parallel = 0$, in the background plasma, where $\omega \sim 2\pi\mathrm{v}_\perp / r_\perp$, and $\omega / k_\parallel$ is equal to the Alfvén velocity $V_{A\infty} = B/(\mu_0 m_i n_\infty)^{1/2}$, Eq. (5) reduces to an equation for the electrostatic potential

$$\frac{\Sigma_\rho}{B}\frac{D\nabla_\perp^2\varphi}{Dt} + \frac{B\nabla_\perp^2\varphi}{\mu_0 V_{A\infty}} = -\frac{2\sin\vartheta}{R}\int_0^{z_c}\frac{\partial p(r,z,t)}{\partial r}dz \quad . \tag{6}$$

To simplify the source term in Eq. (6) we next assume a sharp boundary pressure profile: $\partial p/\partial r = -[p(z,t) - p_\infty]\delta(r - r_\perp)$. Then both inside and outside the cloud the potential satisfies $\nabla_\perp^2\varphi = 0$, with the boundary condition that electric field vanish far away from the cloud since we can ignore the finite extent of the plasma ($r_\perp$ << plasma minor radius). Continuity of φ at the boundary $r = r_\perp$, gives the solutions in each region: $\varphi_{in} = A(t) r \sin\vartheta$, and $\varphi_{out} = A(t) r_\perp^2 r^{-1}\sin\vartheta$. The uniform electric field inside the cloud leads to motion of the

cloudlet as a whole in the $\hat{x}$ direction. The jump conditions across the radius $r_\perp$ admits $A(t)$, and hence the velocity of the cloudlet in the major radius direction is given by

$$\Sigma_\rho \frac{dv_x}{dt} = -\frac{2B^2 v_x}{\mu_0 V_{A\infty}} + \frac{2p_0 L_c}{R}\tilde{\Psi}(t) \tag{7}$$

where we have employed the definitions.

$$\tilde{\Psi}(\tilde{t}) = \int_0^{z_c(t)/L_c} [\tilde{p}(\xi,\tilde{t}) - \beta_\infty/\beta_0]d\xi, \quad \langle\tilde{\Psi}\rangle = \int_0^\infty \tilde{\Psi}(\tilde{t})d\tilde{t} \quad , \tag{8}$$

$\xi = z/L_c$, $\tilde{p} = p(z,t)/p_0$, and $\Sigma_\rho = \Sigma_\rho^{in} + \Sigma_\rho^{out} = m_i[n_0\bar{\tau}L_c + n_\infty z_c(t)] \cong m_i n_0 \bar{\tau} L_c$. Integrating Eq. (7) gives the drift distance of the cloudlet in the direction of increasing R

$$\Delta R = 0.5\beta_0 \kappa_c r_p \frac{V_{A\infty}}{\bar{c}_0}\langle\tilde{\Psi}\rangle \quad . \tag{9}$$

Figure 3 displays $\tilde{\Psi}(\tilde{t})$ versus $\tilde{t}$, varying the two key dimensionless parameters in the parallel dynamics, β_0/β_∞ and Σ_0. Figure 4 shows the dependence of $\langle\tilde{\Psi}\rangle$ with β_0/β_∞ for different values of Σ_0. Using DIII–D inside launch experimental parameters, we find that $V_{A\infty}$ = 5.5 10^6 m/s, and $\kappa_c \approx 20$ from a modification of the channel radius model of Ref. [6], $\beta_0 = 0.024$, β_0/β_∞ = 3.0, Σ_0 = 15, $\bar{c}_0 = 1.5\times10^4$ m/s, and thus $\langle\tilde{\Psi}\rangle$ = 4, and finally ΔR = 17 cm. This result compares well with the shift in the fuel deposition profile towards the magnetic axis measured <1 ms after inside launch pellet injection [2]. The strong scaling of ΔR with β_0, and the larger β_* and thus β_0 expected for pellet clouds in hotter fusion grade plasmas, suggests that low-velocity inside launched pellets may provide a unique solution to refueling problem in fusion reactors. Future work will include the helical effect of the magnetic field on the cloudlet expansion and drift dynamics.

This is a report of work supported by the U.S. Department of Energy under Grant No. DE-FG03-95ER54309.

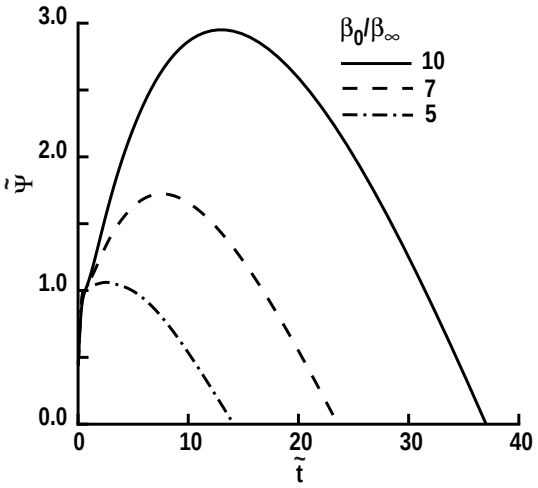

Fig. 3. $\tilde{\Psi}(\tilde{t})$ versus $\tilde{t}$.

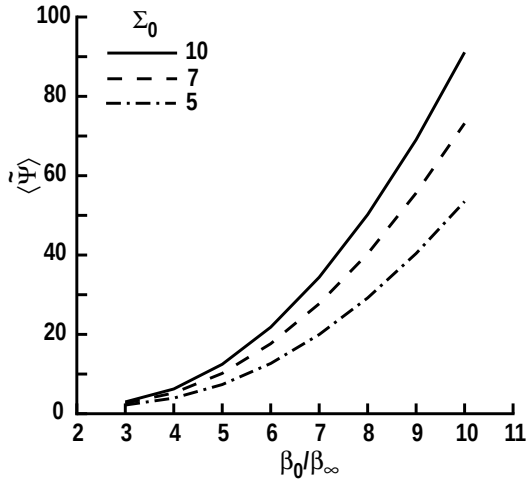

Fig. 4. $\langle\tilde{\Psi}\rangle$ versus β_0/β_∞.

[1] P.T. Lang, K. Buchl, M. Kaufmann, et al., Phys. Rev. Lett. **79**, 1487 (1997).
[2] L.R. Baylor et al., this conference.
[3] P.B. Parks, Plasma Phys. Contr. Fusion **38**, 571 (1996).
[4] I.Yu. Veselova, and V.A. Rozhansky, Sov. J. Plasma Phys. **17,** 817 (1991).
[5] J. de Kloe, et al., Phys. Rev. Lett. **82**, 2685 (1999).
[6] P.B. Parks, Nucl. Fusion **31**, 1431 (1991).